Journal of CO2 Utilization 104 (2026) 103325

Contents lists available at ScienceDirect

Journal of CO2 Utilization

journal homepage: www.elsevier.com/locate/jcou

Growth of ionic polymers on ZIFs to construct core-shell hybrid materials via coordination interactions for catalytic CO_2 conversion

Jinquan Wang [a,*,1], Xiukai Li [a], Siew Ping Teong [a], Shook Pui Chan [a], Zibiao Li [a], Xinglong Zhang [b,*,2], Yugen Zhang [a,*,3]

[a] Institute of Sustainability for Chemicals, Energy and Environment (ISCE2), Agency for Science, Technology and Research (A*STAR), 1 Pesek Road Jurong Island, 627833, Singapore

[b] Department of Chemistry, The Chinese University of Hong Kong, Shatin, New Territories, Hong Kong, China

ARTICLE INFO

Keywords:
ZIFs • Core-shell • hybrid material • Catalysis • CO_2 conversion

ABSTRACT

A sustainable and practical method has been developed for synthesizing ZIF-ionic polymer core-shell hybrid materials. This one-pot, two-step process employs imidazole, zinc nitrate, DABCO (1,4-diazabicyclo[2.2.2]octane), and 1,3,5-tris(bromomethyl)benzene in ethanol, yielding high efficiency. In this approach, DABCO facilitates ZIF formation by deprotonating imidazole and subsequently reacts with 1,3,5-tris(bromomethyl)benzene to generate a poly-DABCO salt that coats the ZIF surface via coordination interactions. The resulting hybrid materials, which exhibit dual Lewis acid and base functionalities, demonstrate exceptional activity and stability in catalyzing CO_2 conversion into cyclic carbonates. Interestingly, the catalyst also exhibits high activity in the synthesis of bis(cyclic carbonate) from diepoxide, which subsequently reacts with diamines to form non-isocyanate polyurethanes. A proposed reaction mechanism, combining experimental findings and density functional theory (DFT) calculations, highlights the critical roles of zinc and the ionic polymer in achieving high catalytic performance. Specifically, zinc and ionic polymer are identified as key contributors to epoxide activation and ring-opening processes. This study not only deepens the understanding of ZIF-polymer hybrid materials but also establishes a strong foundation for future advancements in their design, research, and applications.

1. Introduction

The catalytic conversion of CO_2 into value-added chemicals is regarded as an effective strategy to mitigate CO_2 emissions while advancing sustainable chemical manufacturing [1]. Among the various CO_2 utilization routes, the cycloaddition of CO_2 with epoxides to produce cyclic carbonates has attracted significant interest owing to its 100 % atom economy, mild reaction conditions, and the broad industrial applicability of cyclic carbonates [2]. Zeolitic imidazolate frameworks (ZIFs) and ionic polymers have emerged as efficient heterogeneous catalysts for the cycloaddition of CO_2 and epoxides [3–10]. In particular, integrating ZIFs with ionic polymers represents a promising approach to construct synergistic catalytic systems that combine the complementary advantages of both components. Within such hybrid catalysts, ZIFs can furnish Lewis acidic sites to activate epoxide substrates, while the ionic polymer component provides highly accessible nucleophilic anions that facilitate epoxide ring opening, thereby enhancing the overall catalytic performance.

Zeolitic imidazolate frameworks (ZIFs), a significant subclass of metal-organic frameworks (MOFs), consist of transition metal ions and imidazolate linkers arranged in tetrahedral coordination, mimicking the structure of crystalline aluminosilicate zeolites [11–18]. Their high surface area, stability, and tuneable porosity makes them highly appealing for applications such as heterogeneous catalysis, selective gas adsorption, and separation [19–25]. However, their commercial viability is constrained by high crystallinity, which limits integration into various technologies [26–30]. Additionally, their porous crystalline structure often collapses under mechanical stress, as seen in various

* Corresponding authors.
E-mail addresses: wang_jinquan@a-star.edu.sg (J. Wang), xinglong.zhang@cuhk.edu.hk (X. Zhang), zhang_yugen@a-star.edu.sg (Y. Zhang).
[1] 0000–0001-7076–8056
[2] 0000–0003-1698–692X
[3] 0000–0002-8497–1175

https://doi.org/10.1016/j.jcou.2026.103325
Received 20 November 2025; Received in revised form 29 December 2025; Accepted 7 January 2026
Available online 13 January 2026

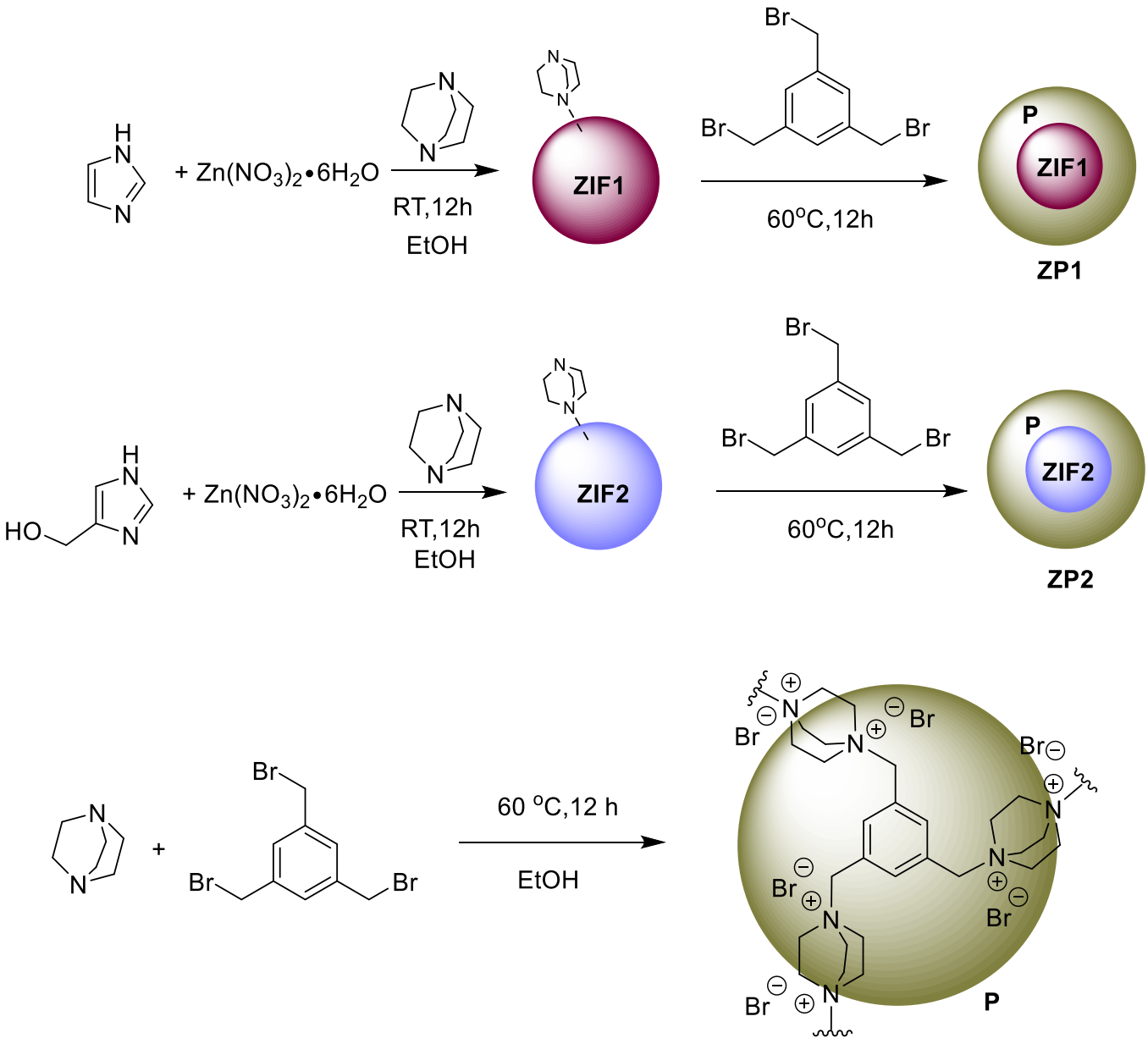

Scheme 1. Synthesis of ZIFs/poly DABCO core-shell hybrid materials and polymer P.

catalytic applications [31–36]. To overcome these challenges, researchers have developed hybrid materials by combining ZIFs with polymers that are flexible, designable, and processable. These hybrids leverage the complementary properties of both components, enhancing processability, stability, and functionality to broaden the applicability of ZIF [37–40].

Several methods have been explored for combining ZIFs (or MOFs) with polymers to create hybrid materials [41], including grafting polymers to and from ZIFs, polymerizing polymers within ZIFs, using polymers as templates for ZIFs, and the bottom-up synthesis of poly-ZIFs. However, these approaches often face challenges due to inherent incompatibilities between the components [42–45]. Additionally, the construction of ZIF-polymer hybrid materials typically involves complex synthesis and separation processes, which hinders their commercial scalability. Developing sustainable and scalable methods for fabricating these materials is essential to unlock their potential for widespread applications [46]. This work centers on the development of a facile, scalable, and eco-friendly approach for fabricating compatible catalytic ZIF-polymer hybrid materials.

A common method for synthesizing ZIFs involves mixing a highly diluted metal salt with organic ligands in an organic solvent and heating the mixture in an autoclave at temperatures up to 200°C [47]. Despite its widespread use, this approach is often time-consuming and energy-intensive. To address these challenges, the addition of organic amines, such as ammonium hydroxide or TEA [48,49], to deprotonate the organic ligands is emerging as a promising method to accelerate the preparation process and reduce energy input. However, most organic amines are toxic, and their environmental impact is often overlooked after the reaction [50,51]. In light of this, we propose that by selecting a suitable amine to deprotonate the imidazole ligand, it could subsequently be used to construct a poly ammonium salt that decorates the surface of the ZIF after synthesis, leading to the formation of ZIF-poly ammonium salt hybrid materials. The key to this design is ensuring that the amine remains on the ZIF surface after synthesis, allowing for polymer growth directly on the surface during polymerization.

With this in mind, we discovered that DABCO, a well-established coordination linker for MOF modification [52–58], can act as an organic base to deprotonate imidazole during ZIF synthesis. DABCO

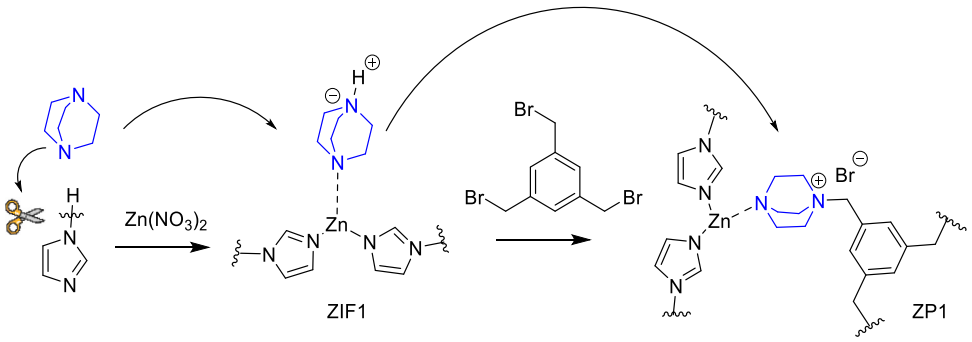

Scheme 2. The design of core-shell synthesis and multifunctional roles of DABCO: 1) Assists in hydrogen removal, 2) Coordinates with ZIF, and 3) Forms an ionic polymer shell.

then reacts with 1,3,5-tris(bromomethyl)benzene to form a poly-DABCO salt, which decorates the surface of the ZIFs (Scheme 1). This poly-DABCO salt grows on the ZIF surface through coordination interactions between DABCO and the ZIFs prior to polymerization. The entire process is a one-pot synthesis of ZIF-ionic polymer core-shell hybrid materials, eliminating the need for separation steps and yielding a highly efficient product. The method is facile, scalable, and environmentally friendly. These novel ZIF-ionic polymer core-shell hybrid materials, incorporating both Lewis acid and base functionalities, hold great promise for the development of functional hybrid materials with diverse applications.

2. Materials and method

2.1. Chemical reagents

All chemical reagents were obtained from Merck and used without additional purification.

2.2. Synthesis of ZP1 and ZP2

Imidazole (6.8 g, 0.10 mol) or 4(5)-(hydroxymethyl)imidazole (9.8 g, 0.10 mol) and $Zn(NO_3)_2{\cdot}6H_2O$ (14.8 g, 0.05 mol) were introduced to a 250 mL flask with 100 mL of ethanol. DABCO (11.2 g, 0.10 mol), pre-dissolved in 100 mL of ethanol, was then added to the mixture, which was stirred at RT for 12 h. After this period, 1,3,5-tris (bromomethyl)benzene (23.8 g, 0.067 mol, with mole ratio to DABCO of 2:3) was introduced, and the temperature was raised to 60 °C. The mixture was heated for an additional 12 h. Upon cooling to RT, a white solid precipitated and was obtained by centrifugation. The product was purified by washing with ethanol, affording a quantitative yield of either ZP1 or ZP2, depending on the imidazole derivative used.

2.3. Synthesis of ionic polymer P

DABCO (0.34 g, 3 mmol) and 1,3,5-tris(bromomethyl)benzene (0.72 g, 2 mmol) were dissolved in 20 mL of ethanol and added to the reaction flask. The reaction was conducted at 60 °C and 12 h. Upon cooling, a white solid precipitated and was obtained by centrifugation. The white solid was then washed by ethanol, affording polymer P in near-quantitative yield.

2.4. Experiments for conversion of CO_2 with epoxide

CO_2 conversion was carried out in a 25 mL stainless-steel reactor. Typically, 1 mmol of glycidyl phenyl ether, 40 mg of ZP, and 2 mL of ethanol were added to the reactor, followed by the introduction of CO_2 at 1.0 MPa. The mixture was then heated to 110 °C and stirred for 4 h. After completion, the reactor was cooled in an ice-water bath, and the residual CO_2 was released slowly. The resulting product was analyzed by gas chromatography (GC) with biphenyl as the internal standard.

2.5. Experiment for production of poly(hydroxylurethane)

1,7-octadiene diepoxide (1 mmol) and hexane-1,6-diamine (1.4 mmol) were mixed in 6 mL of anhydrous DMF in a 25 mL flask. The mixture was then heated at 140 °C under a N_2 atmosphere for 3 days. Upon completion, the resulting product was washed thoroughly with CH_2Cl_2 and dried at 60 °C prior to conduct characterization.

3. Results and discussion

3.1. Core-shell hybrid materials

Our strategy involves the design of ZIF/ionic polymer hybrid materials using a facile, one-pot, two-step green process at a 10-gram scale. In the first step, ZIFs were synthesized by introducing DABCO as a deprotonating agent under RT conditions. In the second step, 1,3,5-tris(bromomethyl)benzene was directly added to the reaction mixture, leading to the formation of a poly-DABCO salt on the ZIF particles. Scheme 2 outlines the multifunctional roles of DABCO and the core-shell formation process, where coordination between DABCO and ZIF likely generates a core-shell structure, with the ZIF core encapsulated within the polymer shell during polymerization. This new method for constructing core-shell structures is straightforward, ensures strong bonding between the core and shell, and does not require additional functional groups for chemical synthesis. The conventional synthesis of ZIF–polymer composites is typically based on physical mixing, in which no specific interaction exists between the ZIF and the polymer matrix. In contrast, DABCO exhibits coordination interactions with the ZIF framework, which not only facilitates the construction of the ionic polymer directly on the ZIF surface but also contributes to the stabilization of the ZIF structure. Scheme 1 depicts the synthesis process for ZIF/poly-DABCO salt hybrid materials and poly-DABCO salts, labelled ZP1, ZP2, and P, with ZP1 and ZP2 incorporating different imidazole. The poly-DABCO salt (P) was synthesized for comparative analysis. Additionally, substituting DABCO with tetramethylethylenediamine for the synthesis of ZIF/ionic polymer hybrids resulted in the polymer failing to grow on the ZIF surface, highlighting the crucial role of DABCO in enabling surface polymerization.

Fig. 1 and Fig. S1 present FESEM and STEM-HAADF results, showcasing the morphology and particle size of the synthesized ZIF-ionic polymer hybrid materials (ZP1 and ZP2) and the ionic polymer (P). The particles display a spherical morphology, with an approximate size of 1 μm. STEM-HAADF images confirm that the ionic DABCO polymer has successfully grown on the ZIF surface, forming a core-shell structure. The FESEM-EDX line scan of Br further confirms the core-shell structure of ZIF and the ionic polymer, demonstrating that the polymer grows on the surface of the ZIF. FESEM-EDX mapping of ZP2 (Fig. S2) reveals the elemental distribution, with distinct colours corresponding to C, N, Zn,

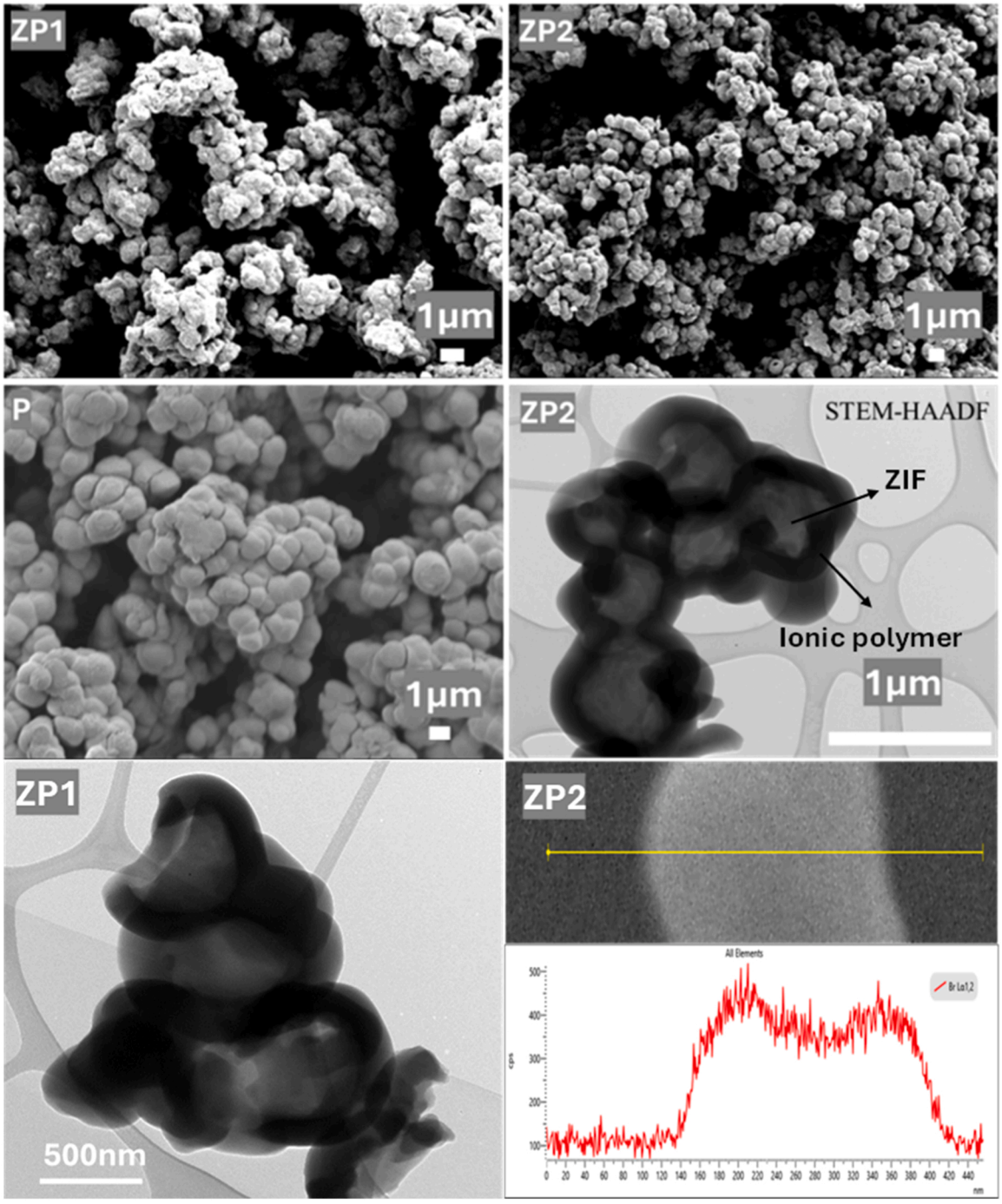

Fig. 1. SEM images of ZP1, ZP2, P and STEM-HAADF images of ZP2.

and Br. Table S1 provides the composition of ZP1-ZP2, determined via ICP-OES and elemental analyses. The Zn contents of ZP1 and ZP2 are 8.01 and 7.63 wt%, respectively. X-ray photoelectron spectroscopy (XPS) further characterizes the elemental composition (Fig. 2). The N1s spectrum shows peaks at 399, 401, and 405 eV, corresponding to C-N, C═N in imidazole, and positively charged quaternary nitrogen in DABCO, respectively [59–63]. The Zn 2p spectra of ZP1 and ZP2, with peaks at 1020.88 and 1044.84 eV, were assigned to Zn $2p^{3/2}$ and Zn $2p^{1/2}$ hybrid orbitals. FT-IR spectra of ZP1 and ZP2 confirm ZIF formation (Fig. S3), with a peak at 430 cm^{-1} for the Zn-N stretching vibration and a peak at 3410 cm^{-1} for -OH stretching in ZP2 [64]. Powder XRD patterns reveal that the ZIF-ionic polymer hybrid materials lack crystallinity (Fig. S4). Thermogravimetric analysis shows that ZP1 and ZP2 are stable up to 200 °C (Fig. S5). The calculated BET surface areas for ZP1 (5 m^2/g), ZP2 (4 m^2/g), and P (4 m^2/g) are very low (Table S2), indicating their non-porous nature. Furthermore, control experiments were conducted to confirm the formation of ZIF-1. The ZIF-1 intermediate coordinated with DABCO was successfully isolated after the first step, and its XRD and FT-IR results consistently verified the formation of ZIF-1 (Fig. 3 and Fig. S6). In the FT-IR spectrum (Fig. S6), a characteristic band at 1674 cm^{-1} corresponds to C═N stretching, confirming the presence of imidazolate-based organic linkers. The band at 1089 cm^{-1} arises from C–H bending vibrations, while the peak at 1496 cm^{-1} is assigned to C═C stretching modes. XPS was further employed to investigate the coordination interaction between ZIF-1 and DABCO (Fig. S7). In the N 1 s spectrum, a distinct peak at ~407 eV is

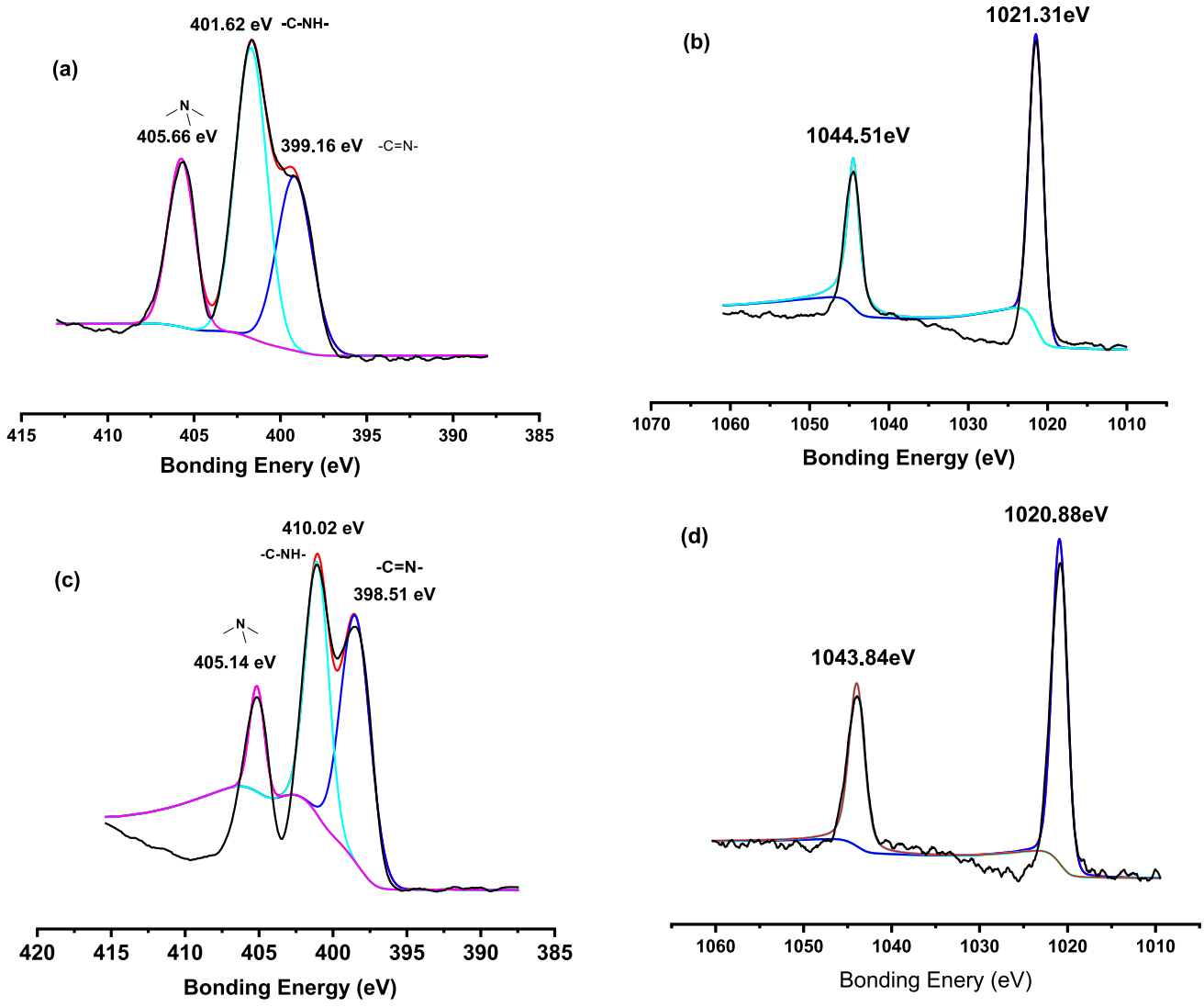

Fig. 2. XPS analysis, (a) ZP1, N, (b) ZP1, Zn, (c) ZP2, N, (d) ZP2, Zn.

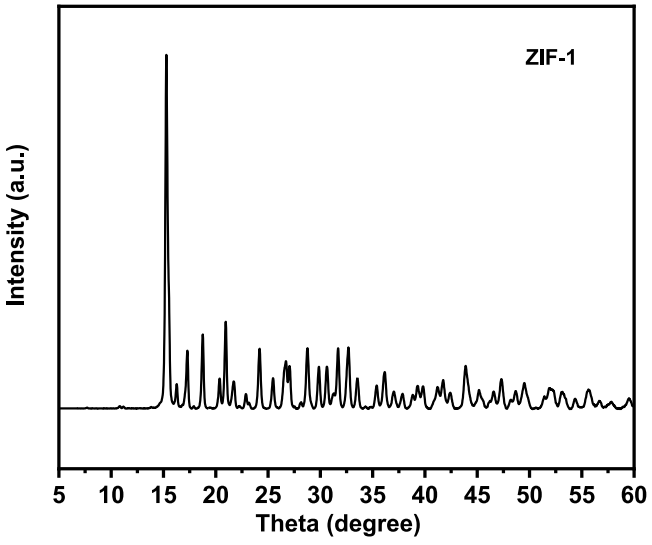

Fig. 3. X-ray diffraction analysis of ZF1.

observed, which is attributed to the C–N species of DABCO, indicating the successful incorporation and coordination of DABCO within the ZIF-1 framework.

Table 1
Screening of catalyst [a].

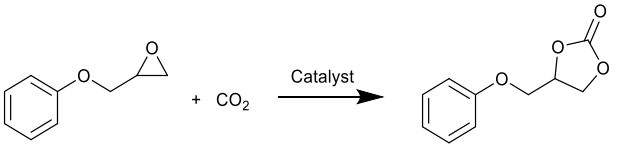

Entry	Catalyst	Conversion[%][b]	Yield[%][b]
1	ZP1	60	59
2	ZP2	83	83
3	ZIF	0	0
4	P	46	46
5[c]	ZP2	70	69
6[d]	ZF2	50	50
7[e]	ZP2	60	60
8 [f]	ZIF2/P	80	80

[a]Reaction condition: 1 mmol glycidyl phenyl ether, 40 mg catalyst, 2 mL EtOH, 10 bar CO_2, 110 °C, 4 h. [b]Conversion and yield were determined by GC. [c]5 bar CO_2. [d]2 bar CO_2. [e]20 mg catalyst. [f]ZIF2

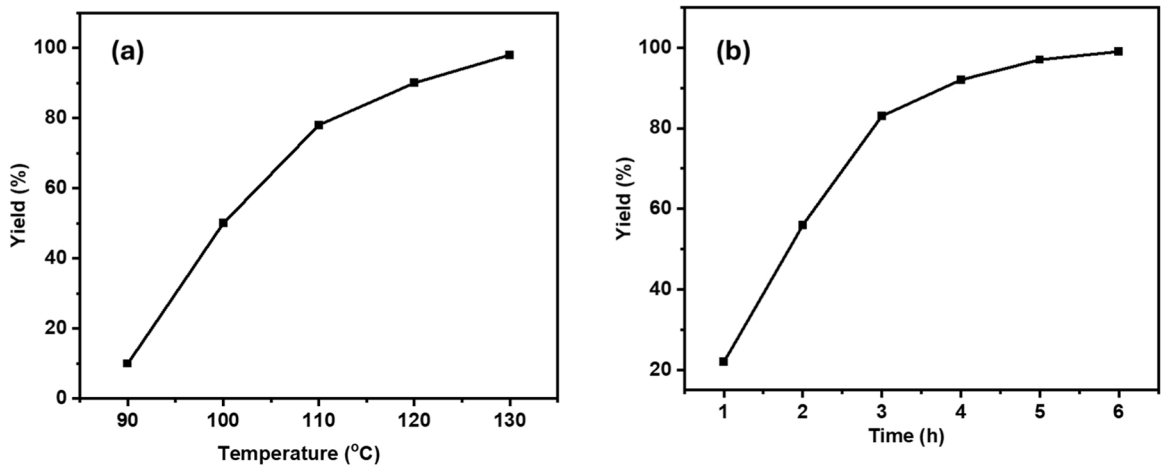

Fig. 4. Study on reaction temperature and kinetic study. (a) Reaction condition: 1 mmol glycidyl phenyl ether, 40 mg ZP2, 2 mL EtOH, 10 bar CO_2, 4 h. Yield was determined by GC. (b) Reaction condition: 1 mmol glycidyl phenyl ether, 40 mg ZP2, 2 mL EtOH, 10 bar CO_2, 110 °C.

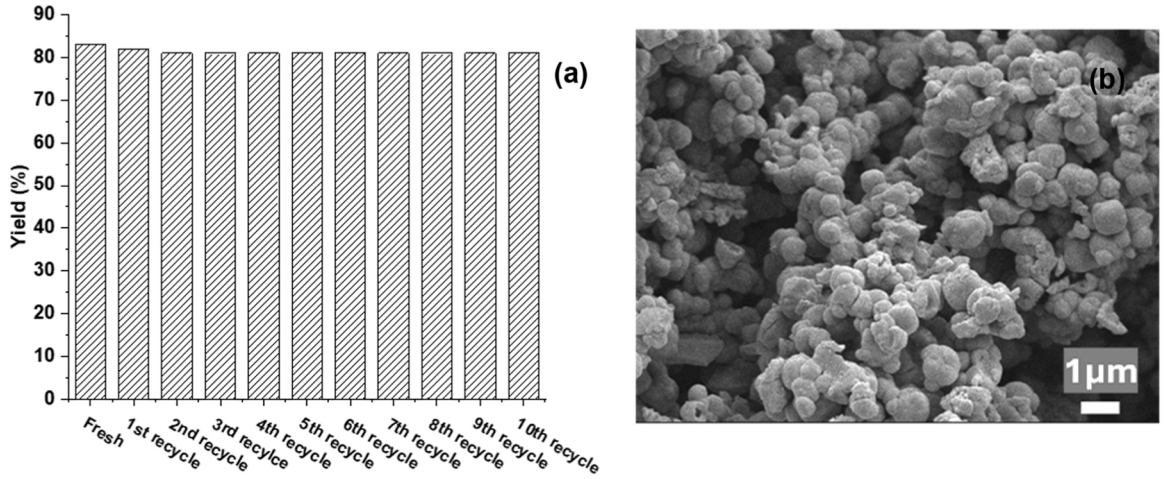

Fig. 5. Recycling of catalyst. (a) Reaction condition: 1 mmol glycidyl phenyl ether, 40 mg ZP2, 2 mL EtOH, 10 bar CO_2, 110 °C, 4 h. Yield was determined by GC. (b) SEM image after recycling.

(20 mg), P (20 mg).

3.2. *Catalytic conversion of CO_2*

ZIF-poly DABCO salt hybrid materials, which combine both Lewis acid and base functionalities, exhibit significant potential for catalysis [65–67]. We demonstrate Lewis acid-Lewis base catalysis in the conversion of CO_2 with epoxides into cyclic carbonates (Table 1). In this reaction, the ZIFs, with Zn acting as a Lewis acid, activate the epoxide, while the poly-DABCO salt, with bromide as a Lewis base, facilitates the ring-opening of the epoxide [68–78]. We first tested ZP1 as a catalyst in ethanol (entry 1, Table 1), yielding cyclic carbonate with a 59 % yield. Previous studies have shown that the hydroxyl group plays a critical role in stabilizing the turnover frequency-determining transition states, thereby promoting the reaction [79–82]. Building on this, we evaluated the catalytic performance of ZP2, which contains a hydroxyl group. Remarkably, ZP2 (entry 2) exhibited higher catalytic activity than ZP1, which can be attributed to its greater density of Lewis acid sites, as confirmed by the NH_3-TPD experiments (Fig. S8). Notably, under the same conditions, ZIF showed no activity (entry 3), emphasizing the critical role of the ionic polymer shell in enhancing activity. Ionic polymer P demonstrated lower activity than ZP1 and ZP2 (entry 4), suggesting that ZIFs, acting as Lewis acids, are essential for promoting the reaction. These results suggest that the ZIF core and the ionic polymer shell in the ZIF-ionic polymer core-shell hybrid materials exhibit a cooperative effect, effectively promoting the reaction between CO_2 and epoxides. A further decrease in pressure and catalyst loading resulted in a noticeable decline in product yield (entries 5–7). In addition, the physical mixture of ZIF2 and polymer P showed slightly lower catalytic activity than ZP2 (entry 8), highlighting the advantage of the integrated hybrid structure.

Reaction temperature and kinetic studies indicate that catalytic activity increases with temperature, ranging from 90°C to 130°C (Fig. 4a), and the reaction is nearly complete after 6 h (Fig. 4b). Further experiments were conducted to study the reusability of the ZIF-poly DABCO core-shell hybrid materials. The results demonstrated the catalyst are stable after 10 cycles with no significant loss of activity (Fig. 5a). The mapping of SEM-EDX analysis revealed no observable changes in particle size, morphology, or elemental distribution before and after recycling (Fig. 5b, Fig. S9), confirming the structural stability of the catalyst. FT-IR spectra of ZP-2 after 10 recycling cycles exhibit no noticeable changes relative to those of the fresh catalyst (Fig. S10), indicating good structural stability during reuse. ICP analysis revealed that the concentration of Zn leached into ethanol after the first reaction was as low as 2 ppm, while after 10 catalytic cycles it further decreased to 1 ppm. This negligible metal leaching accounts for the minimal loss in catalytic activity observed over 10 reuse cycles. As designed, the catalyst of core-shell hybrid material exhibits excellent stability, which can be

Table 2
Substrate scope.[a]).

Entry	Epoxide	Product	Temp. (°C)	Time (h)	Yield (%)[b]
1	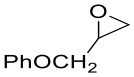	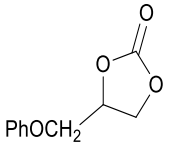	110	4	83
2		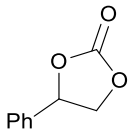	110	16	84
3		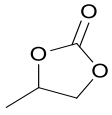	110	6	88
4	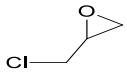	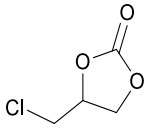	100	6	81
5	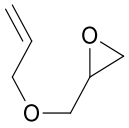	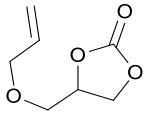	130	8	78
6	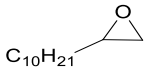	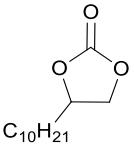	130	72	67
7	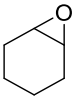	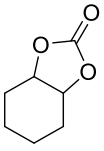	130	24	80

[a]) Conditions: 1 mmol epoxide, 40 mg ZP2, 10 bar CO_2. [b]) Yield was determined by NMR.

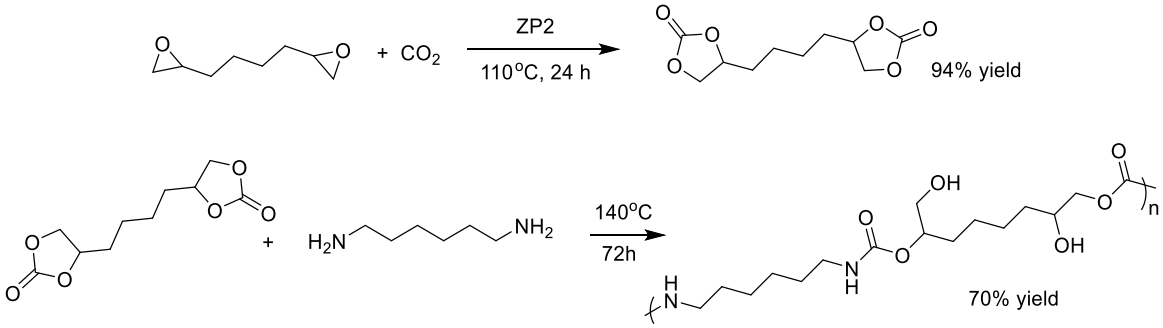

Scheme 3. Synthetic scheme of non-isocyanate polyurethanes.

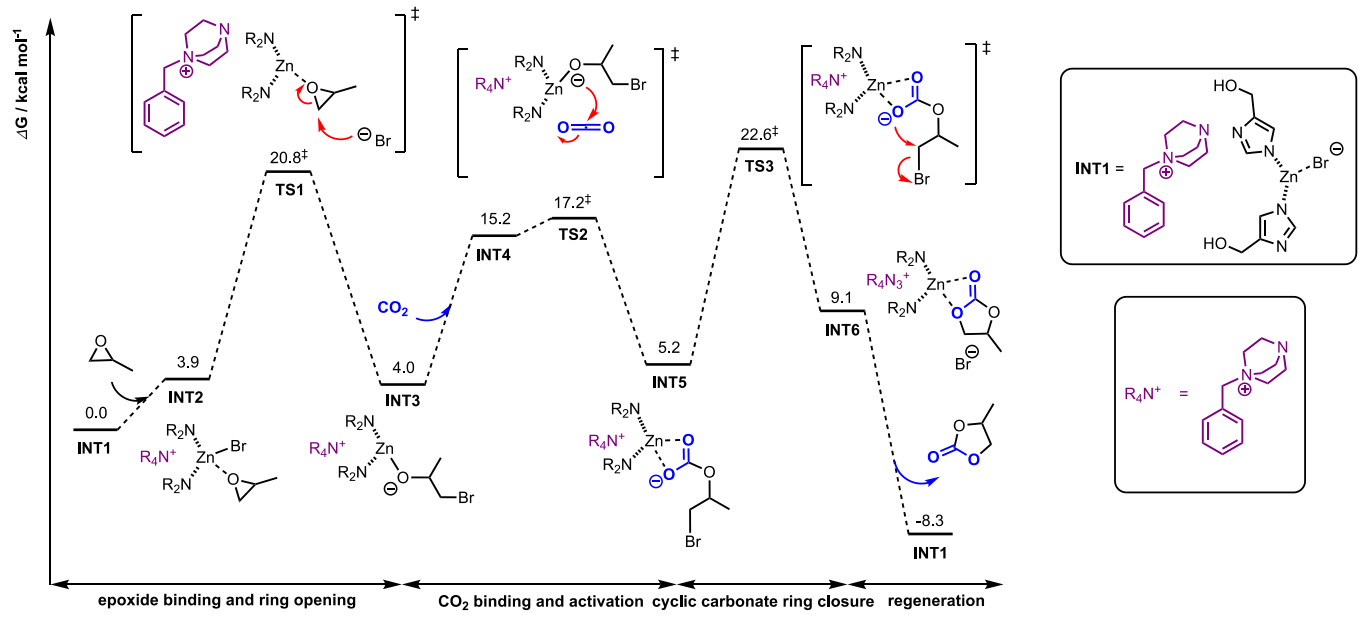

Fig. 6. The Gibbs free energy profile for the formation of cyclic carbonate catalyzed by **ZP2** calculated at SMD(ethanol)-B3LYP-D3BJ/BS2(def2-STZVPD for Br atom and def2-TZVP for others)//B3LYP-D3BJ/BS1(def2-SVPD for Br atom and def2-SVP for others) level of theory. See Fig. S13 for DFT optimized structures of all transition state structures.

attributed to the protective ionic polymer shell and the strong coordination-based bonding between the core and shell.

The ZIF-poly(DABCO) core–shell hybrid materials also act as efficient catalysts for the cycloaddition of CO_2 with a variety of epoxides to afford the corresponding cyclic carbonates (entries 1–4, Table 2). Epoxides bearing alkene functionalities or long hydrophobic chains were well tolerated under the reaction conditions (entries 5 and 6). To further expand the substrate scope, cyclohexene oxide was examined as an internal epoxide, and the catalyst exhibited good activity toward this more challenging substrate. Compared with state-of-the-art catalysts, ZP2 demonstrates competitive catalytic performance (Table S3).

Cyclic carbonates are considered environmentally friendly precursors for non-isocyanate polyurethanes, which are synthesized via polyaddition reactions with amine groups [83]. In this context, our catalyst effectively facilitates the conversion of 1,7-octadiene diepoxide into bis(cyclic carbonate), as illustrated in Scheme 3. The resulting bis (cyclic carbonate) subsequently reacts with hexane-1,6-diamine to form non-isocyanate polyurethane in the absence of a catalyst. The polyurethane product is characterized by FT-IR spectroscopy (Fig. S11). Notably, the characteristic peak at 1783 cm^{-1} , which is corresponding to the C═O stretching vibration of the cyclic carbonate, disappears after polymerization. Meanwhile, a broad peak emerges at 3440 cm^{-1} , attributed to N-H and O-H stretching vibrations from amide and hydroxyl groups, respectively [84]. Additionally, the appearance of peaks at 1664 cm^{-1} further indicates the secondary amide linkages formation within the polyurethane structure. Furthermore, the polyurethane exhibits high stability, remaining stable up to 268 °C (Fig. S12). The fraction of polyurethane solubilized in DMF with 0.5 % LiBr at 70 °C exhibited a molecular weight of 3456 g mol^{-1} .

The reaction mechanism was investigated using Density Functional Theory (DFT) calculations (see Supporting Information section 4.1 for detailed computational methods). The full Gibbs energy profile for the reaction using model catalyst is shown in Fig. 6. The reaction proceeds with firstly the binding of epoxide to Zn metal center, which acts as a Lewis acid activating the epoxide (**INT2**). Subsequently, the epoxide ring is attacked by the bromide anion via S_N2 (**TS1**), with a barrier of 20.8 kcal/mol. The ring-opened species **INT3** then attacks CO_2 carbon (**TS2**), activating it to **INT5**. This is a reversible step, as **INT5** is energetically uphill of **INT3** (by 1.2 kcal/mol) and that the subsequent step of ring closure from **INT5** via **TS3** is more difficult (17.4 kcal/mol) than reverting to **INT3** from **INT5** via **TS2** (12.0 kcal/mol). The ring closure step occurs as the carbonate oxygen anion attacks C–Br in another S_N2 step to yield the cyclic carbonate product coordinated to the catalyst, **INT6**. Finally, the release of the cyclic carbonate regenerates the catalyst **INT1**, thereby continuing the catalytic cycle. The release of cyclic carbonate and thus the overall conversion is exergonically favorable, with a Gibbs energy of reaction ΔG_r = -8.3 kcal/mol. We note that the rate-determining step is the ring closure step (**TS3**), giving an overall barrier of 22.6 kcal/mol (Fig. 6). This agrees well with other theoretical studies on the Zn-based catalysts for the fixation of CO_2 with epoxide, wherein the ring closure step is also shown to be the rate-determining step [49,85,86].

To understand the role of the hydroxyl groups in catalyst **INT1**, we performed further computational studies by replacing the hydroxyl groups in catalyst **INT1** by H atoms (to give **INT1a**, Scheme S2); we also model the **ZP1** catalyst using **INT1b** (Scheme S2). Focusing on the rate-determining step of ring closure, we found that, the ring closure step has a barrier of 23.9 kcal/mol via **TS3a** and 23.6 kcal/mol via **TS3b**, Fig. S14), which is respectively 1.3 and 1.0 kcal/mol higher than **TS3** (Fig. S14). Using simple transition state theory, this predicts that the reaction catalyzed by **INT1** will be kinetically more favored than **INT1a** by about 5.5 times and **INT1b** by 3.7 times. To understand the molecular origins for the roles of OH groups, we performed frontier molecular orbitals (FMOs) and non-covalent interactions (NCI) analysis (Fig. S14). We note that the HOMO and the LUMO for **TS3** and **TS3a** and **TS3b** are similar: the HOMO has highest coefficient on the leaving bromide group and the LUMO has highest coefficients on the aromatic ring of the ammonium cation. The electronic factors are similar for these systems. The NCI plots show that in **TS3**, there is some interaction between the oxygen atom of the OH groups and the C–H bond of the DABCO moiety of the ammonium cations (Fig. S14, circled in green). Additional binding energies between the ammonium cation and the rest of the molecule are −16.6 kcal/mol (single-point SMD(ethanol)-B3LYP-D3BJ/BS2 calculation using the TS geometry) for **TS3**, −14.9 kcal/mol for **TS3a** and −13.7 kcal/mol for **TS3b**. Thus, **TS3** benefits from favorable NCI between the OH groups and the positively charged ammonium cation, thus, lowering the TS barrier and giving better catalyst performance.

To understand the role of ZIF in enhancing the overall catalytic

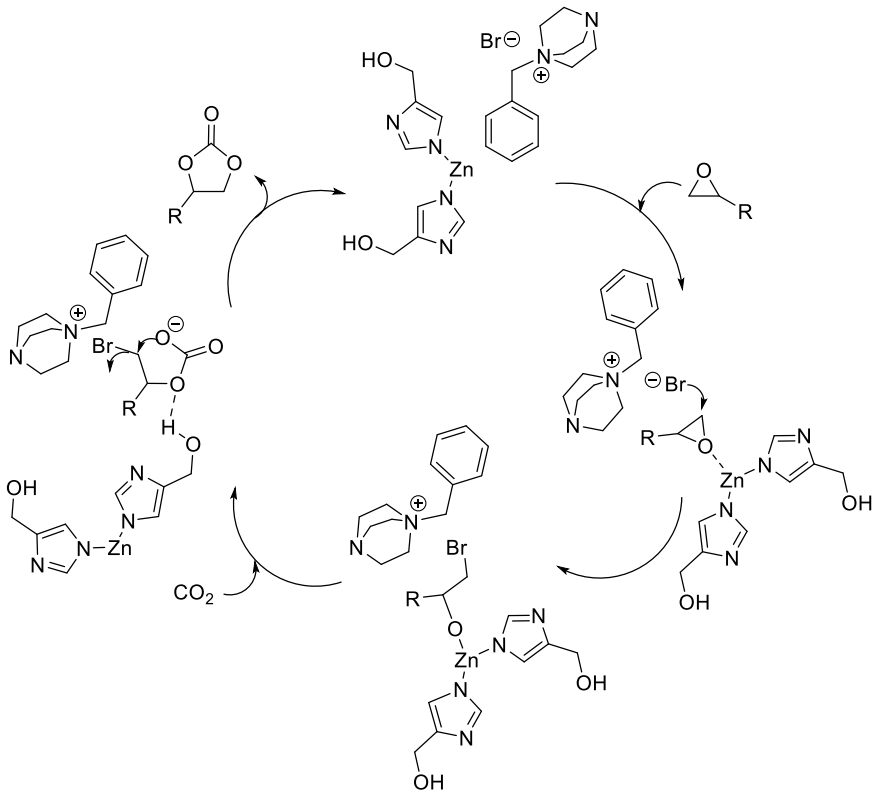

Scheme 4. Proposed reaction mechanism for ZP2-catalyzed conversion of CO_2 with epoxide to cyclic carbonate.

performance of the ZIF/poly ammonium salt composites, we performed the full computational studies on the model system for polymer **P** (Supporting Information section 4.4). We found that in the absence of any Lewis acid activation, the epoxide ring opening step has the highest overall barrier, and the catalytic cycle has an energetic span of 27.9 kcal/mol (Fig. S15). This is 5.3 kcal/mol higher than the model system (Fig. 6). This explains the much reduced conversion and yield when using polymer **P** as a catalyst compared to **ZP2**, which contains Zn ions that are essential in activating epoxide toward nucleophilic attack by the bromide anion.

Based on the experimental results and DFT calculations, we propose a plausible mechanism for cyclic carbonate synthesis, as illustrated in Scheme 4. Initially, the epoxide oxygen coordinates to the Zn metal center, which acts as a Lewis acid, thereby activating the epoxide. Concurrently, the bromide component of **ZP2** attacks the less sterically hindered carbon atom, forming a ring-opened intermediate. This intermediate then undergoes nucleophilic attack on CO_2, resulting in the formation of a carbonate species. Subsequently, ring closure occurs through an S_N2 mechanism, displacing the bromide and yielding the corresponding cyclic carbonate while regenerating the catalyst. The hydroxyl groups in imidazole and the Zn sites in the ZIF framework are crucial for lowering the transition state barrier, which is essential for facilitating the reaction.

4. Conclusion

We have successfully synthesized the first ZIF-ionic polymer core-shell hybrid materials through coordination interactions. These novel materials, which integrate both Lewis acid and base functionalities, demonstrate good catalytic activity and excellent stability for CO_2 conversion. The synthesis employs a one-pot process, eliminating the need for separation steps and producing a quantitative product. This method holds significant promise for the development of new hybrid materials with diverse applications. This work advances the understanding and design of ZIF-polymer hybrid materials and lays the foundation for future research and applications.

CRediT authorship contribution statement

Teong Siewping: Writing – original draft, Methodology, Conceptualization. **Shook Pui Chan:** Writing – original draft, Methodology. **Zibiao Li:** Writing – original draft, Methodology. **Xinglong Zhang:** Writing – original draft, Software, Methodology. **Yugen Zhang:** Writing – review & editing, Writing – original draft, Supervision. **Jinquan Wang:** Writing – review & editing, Writing – original draft, Conceptualization. **Xiukai Li:** Methodology, Data curation.

Declaration of Competing Interest

The authors declare no competing financial interest.

Acknowledgments

This work was supported by the Institute of Sustainability for Chemicals, Energy and Environment (ISCE2), Agency for Science, Technology and Research (A*STAR), Singapore under its RIE2025 Manufacturing, Trade and Connectivity (MTC) MedTech Thematic Grant (Grant No. M24N9b0126), and the National Research Foundation, Prime Minister's Office, Singapore under its Campus for Research Excellence and Technological Enterprise (CREATE) programme (Development of advanced catalysts for electrochemical carbon abatement), Project Code: 370184872. XZ acknowledges the funding support from the Chinese University of Hong Kong (CUHK) under the Vice-Chancellor Early Career Professorship Scheme Research Startup Fund (Project Code 4933634) and Research Startup Matching Support (Project Code 5501779).

Appendix A. Supporting information

Supplementary data associated with this article can be found in the online version at doi:10.1016/j.jcou.2026.103325.

Data availability

No data was used for the research described in the article.

References

[1] Q.W. Song, Z.H. Zhou, L.N. He, Efficient, selective and sustainable catalysis of carbon dioxide, -3228, Green. Chem. 19 (2017) 3707, https://doi.org/10.1039/C7GC00199A.

[2] N. Wei, R.X. Zuo, Y.Y. Zhang, Z.B. Han, X.J. Gu, Robust high-connected rare-earth MOFs as efficient heterogeneous catalysts for CO_2 conversion, Chem. Commun. 53 (2007) 3224–3227, https://doi.org/10.1039/C7CC00363C.

[3] Z.L. Huang, T.X. Zhao, Aqueous-phase synthesis of hollow ZIF-8@poly(ionic liquid) core–shell nanoreactors for enhanced CO_2–epoxide coupling reaction, Chem. Commun. (2026), https://doi.org/10.1039/D5CC06315A.

[4] Z.L. Huang, Y.L. Qu, L. Luo, C.L. Yang, F. Liu, T.X. Zhao, Encapsulation of ZIF-8 within a triazine ion polymer using edge 2-methylimidazole directing effect for enhancing CO_2 fixation into cyclic carbonates via synergistic catalysis, Appl. Surf. Sci. 711 (2025) 164110, https://doi.org/10.1016/j.apsusc.2025.164110.

[5] H. Zhang, W.W. Zhang, F.S. Liu, Z.H. Luo, K.Q. Gao, M.S. Liu, Unveiling the integrated function of metallo-/ionic-covalent organic polymers for boosting atmospheric CO_2 conversion, AIChE J. 70 (2024) e18488, https://doi.org/10.1002/aic.18488.

[6] T.T. Qu, X.R. Duan, Z.W. Ma, F.S. Liu, J.J. Ma, K.Q. Gao, M.S. Liu, Experimental and theoretical investigation of phenylpyridine-based hypercrosslinked polymers for atmospheric CO_2 adsorption and fixation under solvent-/metal-free conditions, Chem. Eng. Sci. 297 (2024) 120298, https://doi.org/10.1016/j.ces.2024.120298.

[7] R. Ping, L. He, Q. Wang, F.S. Liu, H. Chen, S.Z. Yu, K.Q. Gao, M.S. Liu, Unveiling the incorporation of dual hydrogen-bond-donating squaramide moieties into covalent triazine frameworks for promoting low-concentration CO_2 fixation, Appl. Catal. B Environ. 365 (2025) 124895, https://doi.org/10.1016/j.apcatb.2024.124895.

[8] X. Xu, Y. Sui, W. Chen, L. Chai, X. Li, W. Huang, G. Zhou, Y. Li, H. Zhong, Imidazolium-based ionic polymers containing electrostatic and triple hydrogen bond for efficient conversion of CO_2 into cyclic carbonates, ChemCatChem 17 (2025) e202402130, https://doi.org/10.1002/cctc.202402130.

[9] X.H. Xu, Y. Sui, W.T. Chen, X.D. Li, Y.T. Li, H. Zhong, W. Huang, Imidazolium- and triazine-based ionic polymers containing triple hydrogen for efficient conversion of CO_2 into cyclic carbonates under mild conditions, Polymer 337 (2025) 128968, https://doi.org/10.1016/j.polymer.2025.128968.

[10] X. Xu, Y. Sui, W. Huang, W. Chen, X. Li, Y. Li, G. Wang, H. Ye, H. Zhong, Upgraded heterogenization of homogeneous catalytic systems by hollow porous organic frameworks with hierarchical porous shell for efficient carbon dioxide conversion, Asian J. Org. Chem. 11 (2022) e202100727, https://doi.org/10.1002/ajoc.202100727.

[11] B.L. Chen, Z.X. Yang, Y.Q. Zhu, Y.D. Xia, Zeolitic imidazolate framework materials: recent progress in synthesis and applications, J. Mater. Chem. A. 2 (2014) 16811–16831, https://doi.org/10.1039/C4TA02984D.

[12] E. Ploetz, H. Engelke, U. Lachelt, S. Wuttke, The chemistry of reticular framework nanoparticles: MOF, ZIF, and COF materials, Adv. Funct. Mater. 30 (2020) 1909062, https://doi.org/10.1002/adfm.201909062.

[13] S.B. Wang, X.C. Wang, Imidazolium ionic liquids, imidazolylidene heterocyclic carbenes, and zeolitic imidazolate frameworks for CO_2 capture and photochemical reduction, Angew. Chem. Int. Ed. 55 (2016) 2308–2320, https://doi.org/10.1002/anie.201507145.

[14] J.X. Jiang, Y. Shi, M.J. Wu, M. Rezakazemi, T.M. Aminabhavi, R.Z. Huang, C. Jia, S.B. Ge, Biomass-MOF composites in wastewater treatment, air purification, and electromagnetic radiation adsorption-A review, Chem. Eng. J. 494 (2024) 152932, https://doi.org/10.1016/j.cej.2024.152932.

[15] Z.L. Mo, D.Z. Tai, H. Zhang, A. Shahab, A comprehensive review on the adsorption of heavy metals by zeolite imidazole framework (ZIF-8) based nanocomposite in water, Chem. Eng. J. 443 (2022) 136320, https://doi.org/10.1016/j.cej.2022.136320.

[16] Q. Wang, D. Astruc, State of the art and prospects in metal-organic framework (MOF)-based and MOF-derived nanocatalysis, Chem. Rev. 120 (2020) 1438–1511, https://doi.org/10.1021/acs.chemrev.9b00223.

[17] A.E. Baumann, D.A. Burns, B.Q. Liu, V.S. Thoi, Metal-organic framework functionalization and design strategies for advanced electrochemical energy storage devices, Commun. Chem. 2 (2019) 86, https://doi.org/10.1038/s42004-019-0184-6.

[18] T.A. Goetjen, J. Liu, Y.F. Wu, J.Y. Sui, X. Zhang, J.T. Hupp, O.K. Farha, Metal-organic framework (MOF) materials as polymerization catalysts: a review and recent advances, Chem. Commun. 56 (2020) 10109–10418, https://doi.org/10.1039/D0CC03790G.

[19] J.R. Li, R.J. Kuppler, H.C. Zhou, Selective gas adsorption and separation in metal–organic frameworks, Chem. Soc. Rev. 38 (2009) 1477–1504, https://doi.org/10.1039/B802426J.

[20] M.L. Ding, R.W. Flaig, H.L. Jiang, O.M. Yaghi, Carbon capture and conversion using metal–organic frameworks and MOF-based materials, Chem. Soc. Rev. 48 (2019) 2783–2828, https://doi.org/10.1039/C8CS00829A.

[21] C.A. Trickett, A. Helal, B.A. Al-Maythalony, Z.H. Yamani, K.E. Cordova, O. M. Yaghi, The chemistry of metal-organic frameworks for CO_2 capture, regeneration and conversion, Nat. Rev. Mater. 2 (2017) 17045, https://doi.org/10.1038/natrevmats.2017.45.

[22] H. Furukawa, K.E. Cordova, M. O'Keeffe, O.M. Yaghi, The chemistry and applications of metal-organic frameworks, Science 341 (2013) 1230444, https://doi.org/10.1126/science.1230444.

[23] R. Banerjee, A. Phan, B. Wang, C. Knobler, H. Furukawa, M.O'Keeffe, O.M. Yaghi, High-throughput synthesis of zeolitic imidazolate frameworks and application to CO_2 capture, Science 319 (2008) 939–943, https://doi.org/10.1126/science.115251.

[24] N. Stock, S. Biswas, Synthesis of metal-organic frameworks (MOFs): routes to various MOF topologies, morphologies, and composites, Chem. Rev. 112 (2012) 933–969, https://doi.org/10.1021/cr200304e.

[25] R. Freund, O. Zaremba, G. Arnauts, R. Ameloot, G. Skorupskii, M. Dincă, A. Bavykina, J. Gascon, A. Ejsmont, J. Goscianska, M. Kalmutzki, U. Lächelt, E. Ploetz, C.S. Diercks, S. Wuttke, The current status of MOF and COF applications, Angew. Chem. Int. Ed. 60 (2021) 23975–24001, https://doi.org/10.1002/anie.202106259.

[26] S. Begum, Z. Hassan, S. Bräse, M. Tsotsalas, Polymerization in MOF-confined nanospaces: tailored architectures, functions, and applications, Langmuir 36 (2020) 10657–10673, https://doi.org/10.1021/acs.langmuir.0c01832.

[27] T. Kitao, Y.Y. Zhang, S. Kitagawa, B. Wang, T. Uemura, Hybridization of MOFs and polymers, Chem. Soc. Rev. 46 (2017) 3108–3133, https://doi.org/10.1039/C7CS00041C.

[28] G.W. Peterson, D.T. Lee, H.F. Barton, T.H. Epps III, G.N. Parsons, Fibre-based composites from the integration of metal-organic frameworks and polymers, Nat. Rev. Mater. 6 (2021) 605–621, https://doi.org/10.1038/s41578-021-00291-2.

[29] S.S. Nadar, L. Vaidya, S. Maurya, V.K. Rathod, Polysaccharide based metal organic frameworks (polysaccharide–MOF): a review, Coord. Chem. Rev. 396 (2019) 1–21, https://doi.org/10.1016/j.ccr.2019.05.011.

[30] M. Kalaj, M.S. Denny Jr., K.C. Bentz, J.M. Palomba, S.M. Cohen, Nylon-MOF composites through postsynthetic polymerization, Angew. Chem. Int. Ed. 58 (2019) 2336–2340, https://doi.org/10.1002/anie.201812655.

[31] J. Fonseca, T.H. Gong, L. Jiao, H.L. Jiang, Metal–organic frameworks (MOFs) beyond crystallinity: amorphous MOFs, MOF liquids and MOF glasses, J. Mater. Chem. A. 9 (2021) 10562–10611, https://doi.org/10.1039/D1TA01043C.

[32] C.M. Miralda, E.E. Macias, M. Zhu, P. Ratnasamy, M.A. Carreon, Zeolitic imidazole framework-8 catalysts in the conversion of CO_2 to chloropropene carbonate, ACS Catal. 2 (2012) 180–183, https://doi.org/10.1021/cs200638h.

[33] A. Bavykina, N. Kolobov, I.S. Khan, J.A. Bau, A. Ramirez, J. Gascon, Metal-organic frameworks in heterogeneous catalysis: recent progress, mew trends, and future perspectives, Chem. Rev. 120 (16) (2020) 8468–8535, https://doi.org/10.1021/acs.chemrev.9b00685.

[34] V. Pascanu, G.G. Miera, A.K. Inge, B. Martín-Matute, Metal-organic frameworks as catalysts for organic synthesis: a critical perspective, J. Am. Chem. Soc. 141 (2019) 7223–7234, https://doi.org/10.1021/jacs.9b00733.

[35] S. Daliran, A.Reza Oveisi, Y. Peng, A. López-Magano, M. Khajeh, R. Mas-Ballesté, J. Alemán, R. Luque, H. Garcia, Metal-organic framework (MOF)-, covalent-organic framework (COF)-, and porous-organic polymers (POP)-catalyzed selective C-H bond activation and functionalization reactions, Chem. Soc. Rev. 51 (2022) 7810–7882, https://doi.org/10.1039/D1CS00976A.

[36] M.L. Ding, X.C. Cai, H.L. Jiang, Improving MOF stability: approaches and applications, Chem. Sci. 10 (2019) 10209–10230, https://doi.org/10.1039/C9SC03916C.

[37] B.D.S. Deeraj, J.S. Jayan, A. Raman, A. Asok, R. Paul, A. Saritha, K. Joseph, A comprehensive review of recent developments in metal-organic framework/polymer composites and their applications, Surf. Interfaces 43 (2023) 103574, https://doi.org/10.1016/j.surfin.2023.103574.

[38] V.J. Pastore, T.R. Cook, J. Rzayev, Polymer–MOF hybrid composites with high porosity and stability through surface-selective ligand exchange, Chem. Mater. 30 (2018) 8639–9649, https://doi.org/10.1021/acs.chemmater.8b03881.

[39] M. Benzaqui, R. Semino, N. Menguy, F. Carn, T. Kundu, J.M. Guigner, N. B. McKeown, K.J. Msayib, M. Carta, R. Malpass-Evans, C.L. Guillouzer, G. Clet, N. A. Ramsahye, C. Serre, G. Maurin, N. Steunou, Toward an understanding of the microstructure and interfacial properties of PIMs/ZIF-8 mixed matrix membranes, ACS Appl. Mater. Interfaces 8 (2016) 27311–27321, https://doi.org/10.1021/acsami.6b08954.

[40] D.X. Wang, T. Li, Toward MOF@polymer core-shell particles: design principles and potential applications, Acc. Chem. Res. 56 (2023) 462–474, https://doi.org/10.1021/acs.accounts.2c00695.

[41] M. Kalaj, K.C. Bentz, S.A. Jr, J.M. Palomba, K.S. Barcus, Y. Katayama, S.M. Cohen, MOF-polymer hybrid materials: from simple composites to tailored architectures, Chem. Rev. 120 (2020) 8267–8302, https://doi.org/10.1021/acs.chemrev.9b00575.

[42] A. Nishijima, Y. Kametani, T. Uemura, Reciprocal regulation between MOFs and polymers, Coord. Chem. Rev. 466 (2022) 214601, https://doi.org/10.1016/j.ccr.2022.214601.

[43] Y.S. Shi, B. Liang, R.B. Lin, C. Zhang, B.L. Chen, Gas separation via hybrid metal-organic framework/polymer membranes, Trends Chem. 2 (2020) 254–269, https://doi.org/10.1016/j.trechm.2020.01.002.

[44] Y. Lu, H. Zhang, J.Y. Chan, R. Ou, H. Zhu, M. Forsyth, E.M. Marijanovic, C. M. Doherty, P.J. Marriott, M.B. Holl, H.T. Wang, Homochiral MOF-polymer mixed

matrix membranes for efficient separation of chiral molecules, Angew. Chem. Int. Ed. 131 (2019) 17084–17091, https://doi.org/10.1002/ange.201910408.
[45] S.L. Yang, V.V. Karve, A. Justin, I. Kochetygov, J. Espín, M. Asgari, O. Trukhina, D. T. Sun, L. Peng, W.L. Queen, Enhancing MOF performance through the introduction of polymer guests, Coord. Chem. Rev. 427 (2021) 21352, https://doi.org/10.1016/j.ccr.2020.213525.
[46] A. Deacon, L. Briquet, M. Malankowska, F. Massingberd-Mundy, S. Rudić, T. I. Hyde, H. Cavaye, J. Coronas, S. Poulston, T. Johnson, Understanding the ZIF-L to ZIF-8 transformation from fundamentals to fully costed kilogram-scale production, Commun. Chem. 5 (2022) 18, https://doi.org/10.1038/s42004-021-00613-z.
[47] K.S. Park, Z. Ni, A.P. Cote, J.Y. Choi, R. Huang, F.J. Uribe-Romo, H.K. Chae, M. O'Keeffe, O.M. Yaghi, Exceptional chemical and thermal stability of zeolitic imidazolate frameworks, Proc. Natl. Acad. Sci. U. S. A. 103 (2006) 10186–10191, https://doi.org/10.1073/pnas.0602439103.
[48] V.V. Butova, A.P. Budnyk, E.A. Bulanova, C. Lamberti, A.V. Soldatov, Hydrothermal synthesis of high surface area ZIF-8 with minimal use of TEA, Solid State Sci. 69 (2017) 13–21, https://doi.org/10.1016/j.solidstatesciences.2017.05.002.
[49] J.Q. Wang, X.K. Li, G.S. Yi, S.P. Teong, S.P. Chan, X. Zhang, Y.G. Zhang, Noncrystalline zeolitic imidazolate frameworks tethered with ionic liquids as catalysts for CO_2 conversion into cyclic carbonates, ACS Appl. Mater. Interfaces 16 (2024) 10277–10284, https://doi.org/10.1021/acsami.3c19500.
[50] Z.F. Xin, X.S. Chen, Q. Wang, Q. Chen, Q.F. Zhang, Nanopolyhedrons and mesoporous supra-structures of Zeolitic Imidazolate framework with high adsorption performance, Micro Mesopo. Mater. 169 (2013) 218–221, https://doi.org/10.1016/j.micromeso.2012.11.003.
[51] N.A.H.M. Nordin, A.F. Ismail, A. Mustafa, P.S. Goh, D. Ranab, T. Matsuura, Aqueous room temperature synthesis of zeolitic imidazole framework 8 (ZIF-8) with various concentrations of triethylamine, RSC Adv. 4 (2014) 33292–33300, https://doi.org/10.1039/C4RA03593C.
[52] S.G. Kozlova, I.V. Mirzaeva, M.R. Ryzhikov, DABCO molecule in the $M_2(C_8H_4O_4)_2{\cdot}C_6H_{12}N_2$ (M = Co, Ni, Cu, Zn) metal-organic frameworks, Coord. Chem. Rev. 376 (2018) 62–74, https://doi.org/10.1016/j.ccr.2018.07.008.
[53] D. Kim, M. Kang, H. Ha, C.S. Hong, M. Kim, Multiple functional groups in metal-organic frameworks and their positional regioisomerism, Coord. Chem. Rev. 438 (2021) 213892, https://doi.org/10.1016/j.ccr.2021.213892.
[54] A. Bétard, R.A. Fischer, Metal-organic framework thin films: from fundamentals to applications, Chem. Rev. 112 (2012) 1055–1083, https://doi.org/10.1021/cr200167v.
[55] D. Dubbeldam, C.J. Galvin, K.S. Walton, D.E. Elli, R.Q. Snurr, Separation and molecular-level segregation of complex alkane mixtures in metal-organic frameworks, J. Am. Chem. Soc. 130 (2008) 10884–10885, https://doi.org/10.1021/ja804039c.
[56] N. Stock, S. Biswas, Synthesis of metal-organic frameworks (MOFs): routes to various MOF topologies, morphologies, and composites, Chem. Rev. 112 (2012) 933–969, https://doi.org/10.1021/cr200304e.
[57] L. Yan, H.T. Zheng, L. Song, Z.W. Wei, J.J. Jiang, C.Y. Su, Methyl-functionalized flexible ultra-microporous MOF for efficient SF_6/N_2 mixture separation, Chem. Eng. J. 472 (2023) 145145, https://doi.org/10.1016/j.cej.2023.145145.
[58] M.F. de Lange, K.J.F.M. Verouden, T.J.H. Vlugt, J. Gascon, F. Kapteijn, Adsorption-driven heat pumps: the potential of metal-organic frameworks, Chem. Rev. 115 (2015) 12205–12250, https://doi.org/10.1021/acs.chemrev.5b00059.
[59] F. Tian, A.M. Cerro, A.M. Mosier, H.K. Wayment-Steele, R.S. Shine, A. Park, E. R. Webster, L.E. Johnson, M.S. Johal, L. Benz, Surface and stability characterization of a nanoporous ZIF-8 thin film, J. Phys. Chem. C. 118 (2014) 14449–14456, https://doi.org/10.1021/jp5041053.
[60] D.C. Luo, C.R. Chang, Z. Hu, One-step encapsulation of TBAB in ZIF-8 for CO_2 fixation: revealing the synergistic mechanism between TBAB and ZIF-8, ACS Catal. 14 (2024) 11101–11112, https://doi.org/10.1021/acscatal.4c01981.
[61] F. Tian, A.M. Cerro, A.M. Mosier, H.K. Wayment-Steele, R.S. Shine, A. Park, E. R. Webster, L.E. Johnson, M.S. Johal, L. Benz, Surface and stability characterization of a nanoporous ZIF-8 thin film, J. Phys. Chem. C. 118 (2014) 14449–14456, https://doi.org/10.1021/jp5041053.
[62] M. Hayashi, D.T. Lee, M.Dorneles de Mello, J.A. Boscoboinik, M. Tsapatsis, ZIF-8 membrane permselectivity modification by manganese(II) acetylacetonate vapor treatment, Angew. Chem. Int. Ed. 60 (2021) 9316–9320, https://doi.org/10.1002/anie.202100173.
[63] Z. Zhang, H. Zhu, H. Jin, Y. Cao, W. Fang, Z. Zhang, Q. Ma, J. Choi, Y. Li, Restricting linker rotation in nanocages of ZIF-8 membranes using crown ether "molecular locks" for enhanced propylene/propane separation, Angew. Chem. Int. Ed. 64 (2024) e202415023, https://doi.org/10.1002/anie.202415023.
[64] M. Ahmad, R. Patel, D.T. Lee, P. Corkery, A. Kraetz, S.A. Prerna, D. Tenney, X. Nykypanchuk, J.I. Tong, M. Siepmann, J.A. Tsapatsis, Boscoboinik, ZIF-8 vibrational spectra: peak assignments and defect signals, ACS Appl. Mater. Interfaces 16 (2024) 27887–27897, https://doi.org/10.1021/acsami.4c02396.
[65] M. Abdelgaid, G. Mpourmpakis, Structure–activity relationships in Lewis acid–base heterogeneous catalysis, ACS Catal. 12 (2022) 4268–4289, https://doi.org/10.1021/acscatal.2c00229.
[66] Y.Y. Zhang, Y. Jia, M. Li, L.A. Hou, Influence of the 2-methylimidazole/zinc nitrate hexahydrate molar ratio on the synthesis of zeolitic imidazolate framework-8 crystals at room temperature, Sci. Rep. 8 (2018) 9597, https://doi.org/10.1038/s41598-018-28015-7.
[67] C.Q. Wu, Q. Liu, R.R. Chen, J.Y. Liu, H.S. Zhang, R.M. Li, K. Takahashi, P.L. Liu, J. Wang, Fabrication of ZIF-8@SiO_2 micro/nano hierarchical superhydrophobic surface on AZ31 magnesium alloy with impressive corrosion resistance and abrasion resistance, ACS Appl. Mater. Interfaces 9 (2017) 11106–11115, https://doi.org/10.1021/acsami.6b16848.
[68] M.L. Ding, H.L. Jiang, Incorporation of imidazolium-based poly(ionic liquid)s into a metal–organic framework for CO_2 capture and conversion, ACS Catal. 8 (2018) 3194–3201, https://doi.org/10.1021/acscatal.7b03404.
[69] J.Q. Wang, W. Sng, G. Yi, Y.G. Zhang, Imidazolium salt-modified porous hypercrosslinked polymers for synergistic CO_2 capture and conversion, Chem. Common 51 (2015) 12076–12079, https://doi.org/10.1039/C5CC04702A.
[70] J.Q. Wang, J.G.W. Yang, G. Yi, Y.G. Zhang, Phosphonium salt incorporated hypercrosslinked porous polymers for CO_2 capture and conversion, Chem. Common 51 (2015) 15708–15711, https://doi.org/10.1039/C5CC06295K.
[71] J.Q. Wang, Y.G. Zhang, Facile synthesis of N-rich porous azo-linked frameworks for selective CO_2 capture and conversion, Green. Chem. 18 (2016) 5248–5253, https://doi.org/10.1039/C6GC01114D.
[72] W. Xu, H. Chen, K.C. Jie, Z.Z. Yang, T.T. Li, S. Dai, Entropy-driven mechanochemical synthesis of polymetallic zeolitic imidazolate frameworks for CO_2 fixation, Angew. Chem. Int. Ed. 58 (2019) 5018–5022, https://doi.org/10.1002/anie.201900787.
[73] J.Q. Wang, Y.G. Zhang, Boronic acids as hydrogen bond donor catalysts for efficient conversion of CO_2 into organic carbonate in water, ACS Catal. 6 (2016) 4871–4876, https://doi.org/10.1021/acscatal.6b01422.
[74] T.K. Pal, D. De, P.K. Bharadwaj, Metal-organic frameworks for the chemical fixation of CO_2 into cyclic carbonate (No), Coord. Chem. Rev. 408 (2020) 213173, https://doi.org/10.1016/j.ccr.2019.213173.
[75] C. Martin, G. Fiorani, A.W. Kleij, Recent advances in the catalytic preparation of cyclic organic carbonates, ACS Catal. 5 (2015) 1353–1370, https://doi.org/10.1021/cs5018997.
[76] G. Fiorani, W. Guo, A.W. Kleij, Sustainable conversion of carbon dioxide: the advent of organocatalysis, Green. Chem. 17 (2015) 1353–1389, https://doi.org/10.1039/C4GC01959H.
[77] M. Mikkelsen, M. Jorgensen, F.C. Krebs, The teraton challenge. A review of fixation and transformation of carbon dioxide, Energy Environ. Sci. 3 (2010) 43–81, https://doi.org/10.1039/B912904A.
[78] Q.W. Song, Z.H. Zhou, L.N. He, Efficient, selective and sustainable catalysis of carbon dioxide, Green. Chem. 19 (2017) 3707–3728, https://doi.org/10.1039/C7GC00199A.
[79] B.H. Xu, J.Q. Wang, J. Sun, Y. Huang, J.P. Zhang, X.P. Zhang, S.J. Zhang, Fixation of CO_2 into cyclic carbonates catalyzed by ionic liquids: a multi-scale approach, Green. Chem. 17 (2015) 108–122, https://doi.org/10.1039/C4GC01754D.
[80] J.Q. Wang, J.Y. Leong, Y.G. Zhang, Efficient fixation of CO_2 into cyclic carbonates catalysed by silicon-based main chain poly-imidazolium salts, Green. Chem. 16 (2014) 4515–4519, https://doi.org/10.1039/C4GC01060D.
[81] J.Q. Wang, J. Sun, W.G. Cheng, K. Dong, X.P. Zhang, S.J. Zhang, Experimental and theoretical studies on hydrogen bond-promoted fixation of carbon dioxide and epoxides in cyclic carbonates, Phys. Chem. Chem. Phys. 14 (2012) 11021–11026, https://doi.org/10.1039/C2CP41698K.
[82] C.J. Whiteoak, A. Nova, F. Maseras, A.W. Kleij, Merging sustainability with organocatalysis in the formation of organic carbonates by using CO_2 as a feedstock, ChemSusChem 5 (2012) 2032–2038, https://doi.org/10.1002/cssc.201200255.
[83] L. Maisonneuve, O. Lamarzelle, E. Rix, E. Grau, H. Cramail, Isocyanate-free routes to polyurethanes and poly(hydroxy urethane)s, Chem. Rev. 115 (2015) 12407–12439, https://doi.org/10.1021/acs.chemrev.5b00355.
[84] J. Byun, K.A.I. Zhang, Controllable homogeneity/heterogeneity switch of imidazolium ionic liquids for CO_2 utilization, ChemCatChem 10 (2018) 4610–4616, https://doi.org/10.1002/cctc.201801086.
[85] L. Wang, T. Huang, C. Chen, J. Zhang, H. He, S. Zhang, Mechanism of hexaalkylguanidinium salt/zinc bromide binary catalysts for the fixation of CO_2 with epoxide: A DFT investigation, J. CO_2 Util. 14 (2016) 61–66, https://doi.org/10.1016/j.jcou.2016.02.006.
[86] F.M. Al-Qaisi, A.K. Qaroush, K.I. Assaf, A.F. Eftaiha, I.K. Okashah, A.H. Smadi, F. Alsoubani, A.S. Barham, T. Repo, Sustainable synthesis of cyclic carbonates from CO_2 using zinc adeninium bromide as a biorenewable, Inorg. Chim. Acta 557 (2023) 121716, https://doi.org/10.1016/j.ica.2023.121716.